Studying Kenaf Core Drying Uniformity in a Tray Dryer Through CFD

S. Misha, S. Mat, M.A.M. Rosli, M.H. Ruslan, E. Salleh, and K. Sopian

Abstract— Application of tray dryer is widely used in agricultural drying because of its simple design and capability to dry products at high volume. However, the greatest drawback of the tray dryer is uneven drying because of poor airflow distribution in the drying chamber. Implementing the proper design of a tray dryer system may eliminate or reduce non-uniformity of drying and improves drying performance. This study investigates kenaf core drying uniformity in a tray dryer through Computational Fluid Dynamics (CFD) simulation. The simulation focused on air velocity above the products and was conducted under steady state condition to simplify the analysis. Product trays were assumed to be porous media for airflow. The experimental and simulation data exhibit very good agreement. The drying rate of dried products in each tray was predicted based on average air velocity from the simulation. The result shows that, the higher the air velocity, the higher the drying rate of the products. The alternate arrangement of tray position was adopted to ensure that all trays are exposed directly to drying air and to improve airflow distribution in drying chamber. There was a variation of final moisture content for product at different columns. As the distance of product far from the air inlet, the air velocity decreased. However the uniformity of air flow distribution to each level of product at the same column are acceptable. CFD simulation is very useful to predict the airflow distribution throughout the drying chamber with reliable results and cheaper cost. Drying using semi-continuous mode was recommended to improve drying time and uniformity.

Keywords— Tray dryer, drying simulation, kenaf core drying.

Suhaimi Misha is with the Faculty of Mechanical Engineering, Universiti Teknikal Malaysia Melaka, Hang Tuah Jaya, 76100 Durian Tunggal, Melaka (e-mail:suhaimimisha@ utem.edu.my).

Sohif Mat is with the Solar Energy Research Institute, Universiti Kebangsaan Malaysia, 43600 Bangi, Selangor, Malaysia (e-mail: drsohif@gmail.com)

Mohd Afzanizam Mohd Rosli is with the Faculty of Mechanical Engineering, Universiti Teknikal Malaysia Melaka, Hang Tuah Jaya, 76100 Durian Tunggal, Melaka (e-mail:afzanizam@ utem.edu.my).

Mohd Hafidz Ruslan is with the Solar Energy Research Institute, Universiti Kebangsaan Malaysia, 43600 Bangi, Selangor, Malaysia (e-mail: hafidzruslan@gmail.com)

Elias Salleh is with the Solar Energy Research Institute, Universiti Kebangsaan Malaysia, 43600 Bangi, Selangor, Malaysia (e-mail: elsall06@gmail.com).

Kamaruzzaman Sopian is with the Solar Energy Research Institute, Universiti Kebangsaan Malaysia, 43600 Bangi, Selangor, Malaysia (e-mail: ksopian@eng.ukm.my)

I. Introduction

Tray dryers are the most widely used dryers for various drying applications because of their simple design and low cost. Generally, a tray dryer consists of several stacks of trays placed in an insulated chamber in which hot air is distributed by a fan or natural flow. The uniformity of airflow distribution over the trays is crucial to obtain uniform product quality. The variation of the final moisture content of the dried product at different tray positions is commonly encountered because of poor airflow distribution [1]. In a conventional tray dryer, the hot air inlet is usually located at the bottom and the air passes through the others trays. Thus, the products located on the bottom trays are more dried than those on the upper trays, which are subjected to decreased temperature and air velocity. This is one of the reason why producers are not interested in using conventional tray dryers [2],[3]. This problem also limits the volume of the product to be loaded in the dryer system. Generally, drying air temperature and velocity significantly affect drying rate [4],[5].

Measuring the drying parameters in the drying chamber is expensive, difficult, and time consuming because sensors and data loggers have to be installed in several positions, particularly in a large-scale dryer. Therefore, CFD simulation is used extensively in drying analysis because of its ability to solve systems of differential equations for the conservation of mass, momentum, and energy with the use of advanced numerical methods to predict temperature, velocity, and pressure profiles in the drying chamber. CFD is considered an integral part of engineering design and analysis because it can predict the performance of new system designs.

Mathioulakis et al. [2] developed an industrial batch-type tray dryer for drying fruits. They used CFD simulation to predict the air velocity profiles in the drying chamber and found that the final moisture content in several trays was not uniform. Comparison of the CFD simulation result and the experimental data revealed a strong correlation between drying rate and air velocity. Margaris and Ghious [6] studied the numerical simulation inside a drying chamber. A set of measurements was obtained experimentally above a single tray to validate the model. The validation of the measured data and the simulation results through CFD showed that the standard k–e model is the most adequate turbulence model. Tzempelikos et al. [7] predicted the 3D flow problem through

Nomenclature		
C, D	prescribed matrices	σ_k
C_0, C_1	empirical coefficients	σ_ε
C_{ij}	prescribed matrices	*E* to
D_{ij}	mass diffusion coefficient	v_i ve
ρ	density of fluid	v_{mag}
k	turbulent kinetic energy	$(\tau_{ij})_e$

the solution of the steady-state incompressible, Reynolds-Averaged Navier-Stokes (RANS) equations with the incorporation of the standard k-ε turbulence model. The two-phase flow based on mixture model also can be simulated by CFD software FLUENT [8].

Kenaf application is an alternative for wood-based application. Kenaf stem produce two types of fibers: a coarser fiber in the outer layer and a finer fiber in the core. In producing the kenaf fiber, both fibers need to be dried. Kenaf fibres have been commercially used as industrial fibres in various industries such as in the fibre board, paper, mattress, thermoplastic composites, cushion, insulator, wall panels, door and etc. The drying kinetic of thin layered kenaf core at different drying conditions has been studied by Misha et al. [9], who found that the Two-Term model is the best model in describing the drying curves of the kenaf core. This study aims to design and evaluate an industrial-scale tray dryer for chipped kenaf core. CFD is used to predict airflow distribution in the drying chamber to study drying uniformity. Uniform airflow distribution in drying chambers affects the efficiency and homogeneity of the products being dried. The use of desiccant material in drying applications also improves the uniformity of the dried product [10].

II. METHOD AND SIMULATION

A. Dryer System

The industrial scale of solar assisted solid desiccant dryer was designed and developed to investigate system performance and drying uniformity in the drying chamber. The experiment setup has been discussed by Misha et al. [11]. However some improvement have been carried out to produce better drying air condition. The new schematic diagram of the experimental setup as shown in Fig. 1. The suggestion of

dryer system improvement to connect solar collector directly to heat exchanger 1 and 2 were obtained from the previous work [12]. In this experiment both electrical heaters were not used because of high solar radiation along the drying process. The details experimental setup was not discussed in this paper since the focus of this paper to study the airflow distribution in the drying chamber. Fig. 2 shows the illustration of the experimental setup.

The design of the drying chamber is shown in Fig. 3, and includes seven layers of trays, with each layer comprising six trays with dimensions of 64 cm x 92 cm each, for a total of 42 trays. When viewed from the side, only 21 trays are visible, with the remainder visible on the other side. The drying chamber is designed symmetrically from the top view. The sensors are installed only at the right side, assuming that values from the left side are the same, owing to this symmetry. The volume of the drying chamber is 1.7 m (height) x 2 m (width) x 3 m (length). The wall of the dryer system was constructed using 6-cm thick hollow polycarbonate with a hollow space in the middle, 4 cm deep. The top roof is made of glass. The middle trays were positioned between the trays in the first and third columns. This tray arrangement was adopted to ensure that all trays are exposed directly to drying air and to improve airflow distribution throughout the drying chamber. In a conventional arrangement (straight position), the trays in the first column blocks the drying air from the trays in the second and third columns, which reduces drying performance. The design of drying chamber allow drying air flows from inlet to outlet without any obstacle objects. This is to ensure all the products exposed directly to drying air and improve drying performance and uniformity.

Five random positions (A10 to A14) in the drying chamber, inlet (A4) and outlet (A5) of the drying chamber
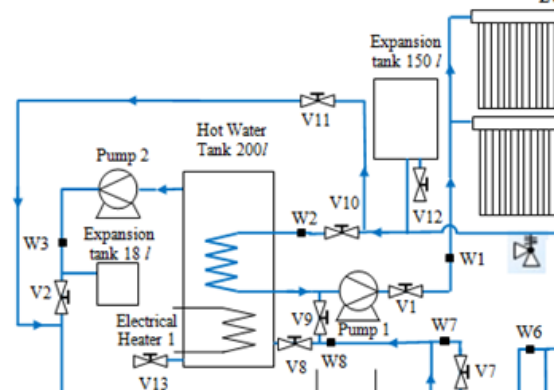
Legends : → Water flow ■ Position of water sensor
→ Air flow ● Position of air sensor

Fig. 1 Schematic diagram of the experiment.

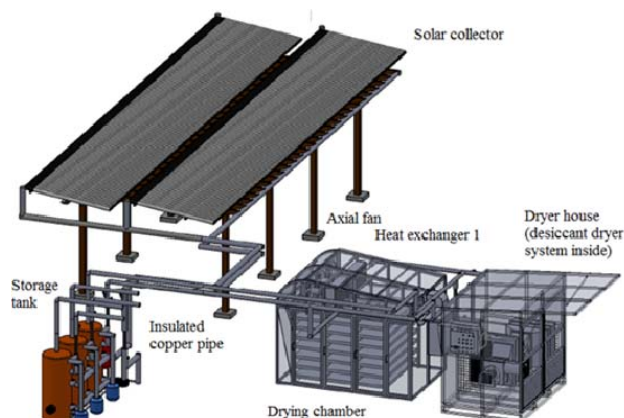Fig. 3 Drying chamber design.

Fig. 2 Illustration of experimental setup.

were selected to be installed with velocity, temperature, and humidity sensors, as shown in Fig. 4. The load cell was also installed to trays 4, 9, 11, 13, and 18 to monitor weight loss. The detailed specifications of the sensors are shown in Table 1. The sensors at others position were not discussed because the focus of this paper is only on airflow distribution in the drying chamber. The actual picture of drying chamber and dryer system as shown in Fig. 5.
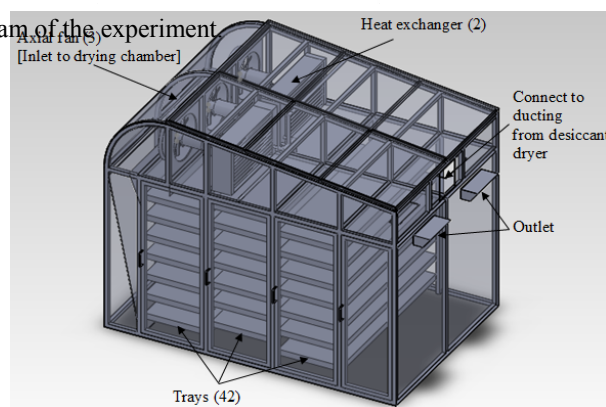
Table 1 Characteristic of measuring instruments

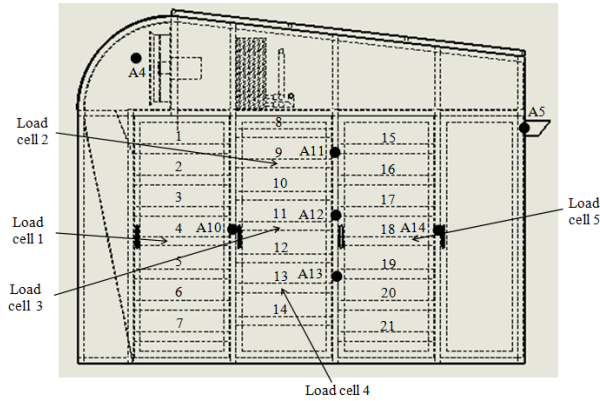| No	Instruments	Properties	Range	Accuracy	Uncertainty
1	Air humidity sensor	0-10V, 4-20mA	5 - 95% RH	±3%	±1%
2	Temperature sensor (IC AD595C)	10mV/°C	-55 - 125	±1°C	±0.75
3	Velocity sensor	1mV/m/s	0.4 - 30 m/s	±(2%+0.1 mV)	±0.01 m/s
4	Load cell	2mv/V	0 - 10 kg	±0.02 kg	±0.012 kg

Fig. 4 Sensors position

Fig. 5   Drying chamber and dryer system

B. Material

The kenaf core fiber was supplied by Lembaga Kenaf and Tembakau Negara (LKTN). The kenaf core samples as shown in Fig. 6. The sample of the kenaf core fiber is a very light material with a density of approximately 100 kg/m3. The total weight of the sample in all trays is approximately 155

Fig. 6   Chipped kenaf core fibre

kg. The core fiber is dried without the outer layer and was chipped. The thickness of the product on the tray is approximately 6 cm. The initial moisture content was determined by oven-drying at 105 °C until constant weight was obtained [13]. The average initial moisture content of the sample was approximately 55% wet basis.

C.   Basic governing equations for CFD simulation

The mass, momentum and energy conservation of drying air result in the continuity, Navier-Stokes and energy equation, respectively [14]. The turbulent model is used in this CFD simulation. The turbulent kinetic energy, k, and its rate of dissipation, ε, are calculated from the following transport equations :

$$\frac{\partial}{\partial t}(\rho k) + \frac{\partial}{\partial x_i}(\rho k u_i) = \frac{\partial}{\partial x_j}\left[\left(\mu + \frac{\mu_t}{\sigma_k}\right)\frac{\partial k}{\partial x_j}\right] G_k +$$
$$G_b - \rho\varepsilon - Y_M + S_k \tag{1}$$

$$\frac{\partial}{\partial t}(\rho\varepsilon) + \frac{\partial}{\partial x_i}(\rho\varepsilon u_i) = \frac{\partial}{\partial x_j}\left[\left(\mu + \frac{\mu_t}{\sigma_\varepsilon}\right)\frac{\partial\varepsilon}{\partial x_j}\right] +$$
$$C_{1\varepsilon}\frac{\varepsilon}{k}(G_k + C_{3\varepsilon}G_b) - C_{2\varepsilon}\rho\frac{\varepsilon^2}{k} + S_\varepsilon \tag{2}$$

Convective heat and mass transfer modeling in the k -ε models is given by the following equation [15]:

$$\frac{\partial}{\partial t}(\rho E) + \frac{\partial}{\partial x_i}[u_i(\rho E + p)]$$
$$= \frac{\partial}{\partial x_i}\left[\left(k + \frac{c_p\mu_t}{Pr_t}\right)\frac{\partial T}{\partial x_i} + u_i(\tau_{ij})_{eff}\right] + S_h \tag{3}$$

Product trays are assumed to be porous media for airflow. Porous media are modeled by adding a momentum source term to the standard fluid flow equations. The source term is composed of two parts: a viscous loss term and an inertial loss term.

$$S_i = -\left(\sum_{j=1}^{3} D_{ij}\mu v_j + \sum_{j=1}^{3} c_{ij}\frac{1}{2}\rho v_{mag}v_i\right) \tag{4}$$

D. Simulation details

The numerical finite volume method used in Fluent 14.0 was used to solve Eq. (1) to (4) and to build a numerical model based on an unstructured 3D mesh using tetrahedral cells. Navier-Stokes equations and continuity equation also can be solved numerically by finite element method as reported by Chuchard et al. [16]. Mesh adaption was performed in this simulation to ensure that the solution was mesh independent and to obtain accurate results. The numbers of cells, faces, and nodes before and after mesh adaption is shown in Table 2.

The meshing of the drying chamber as shown in Fig. 7. The simulation was conducted under steady state condition because the study focused on the pattern of the air stream in the drying chamber.

Table 2 Number of cell, face and nodes in CFD
        simulation

No.	Elements	Original	Adapt	Change
1	Cell	2484849	2503056	18207
2	Face	4988438	5032709	44271
3	Nodes	427870	435358	7488

The boundary conditions are shown in Fig. 8. The boundary conditions were set up as follows:

- Inlet 1: The air mass flow rate was 0.29 kg/s (approximate velocity of 1.5 m/s normal to air inlet), and the air temperature was 56 °C.
- Inlet 2: The air mass flow rate was 0.145 kg/s (50% of inlet 1 but has the same velocity of 1.5 m/s), and the air temperature was 56 °C.
- Outlet: The gauge pressure was assumed to be equal to 0 at the outlet.
- Porous media: The trays were assumed to be porous with 10% porosity.
- Wall: The heat transfer coefficient of the chamber wall is 4 W/(m^{2}K) and environmental conditions were defined. The environmental temperature was assumed to be 34 °C, and the temperature at the roof top is 45 °C (contact with the heat source from radiation). The bottom surface was assumed to have no heat loss. Only half of the drying chamber was analyzed because its shape was made symmetrical by defining the symmetry surface to the middle boundary.
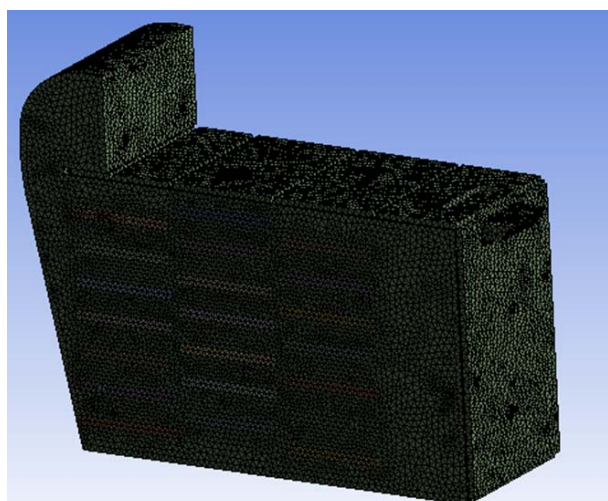

Fig. 7 Meshing of drying chamber space

Misha et al. [17] was study comparison between porous and solid product, it was found that by using porous product the overall velocities in the drying chamber are lower than solid product since some of the hot air stream pass through the porous product. Tzempelikos et al. [18] investigated the airflow distribution inside the batch-type tray air dryer through a commercial CFD package. In the simulation, the tray used inside the drying chamber, was modeled as a thin porous media of finite thickness.
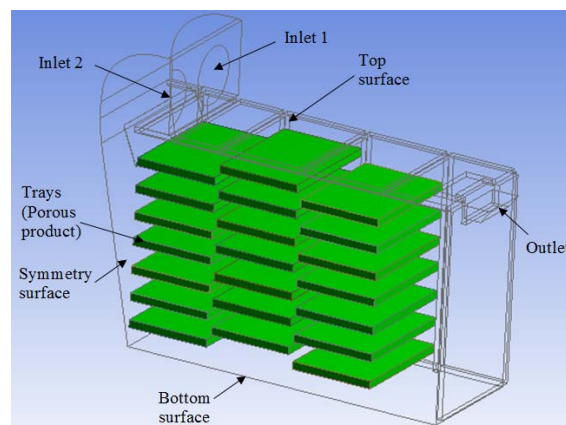

Fig. 8 Drying chamber layout and boundary
         conditions.

III. RESULT AND DISCUSSION

The drying experiment was conducted in one days with average solar radiation of 834 W/m^2. The drying was begun at approximately 10.30 am and was stopped at 2.15 pm. The experiment was stopped when the samples in first column of samples achieved moisture content below 15% wet basis. Actually the experiment was continue until all samples in the drying chamber achieve moisture content below 15% by remove the dried sample (first column) and shift the second and third column of samples to the first and second column, respectively. However for the validation purpose, only the first experiment data required because at the initial stage all the products have similar moisture contents. The graph of moisture contents against time for five trays as shown in Fig. 9.

Variations of final moisture content were observed along the experiment. The highest drying rate was at tray 4, followed by trays 13, 11, 9, and 18. The average inlet air velocity at point A4 is 1.5 m/s and the average outlet air velocity at point A5 is approximately 8.9 m/s. The sensors were installed approximately 3 cm from the product level in the tray and the position can't be adjusted. The drying air in this region should carry moisture because of its proximity to the product. The average temperature and absolute humidity in the drying chamber is shown in Table 3.
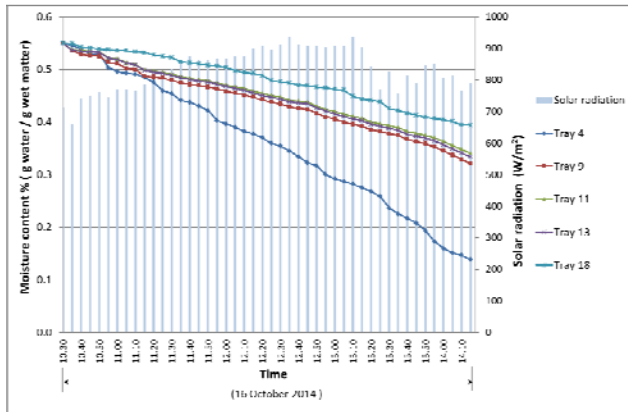
Fig. 9 Moisture contents against time

It was found that, the tray at the first column, which is close to the air inlet, was experience higher air velocity, followed by the second and third columns. When the moisture content of the sample is high, the drying rate is strongly influenced by air velocity. The drying rate for trays number 9, 11, and 13 is approximately the same because all trays were located at second column. Tray 18 only achieved 39% moisture content at the end of the experiment. The variation of final moisture contents for selected trays as shown in Table 4. Semi continuous mode is required to dry product in second and third column. The dried product in the first column should be removed and shifted the product in second and third column to first and second column, respectively. However for validation purpose with CFD simulation, only the first experiment was reported. This study focused on drying uniformity; thus, the performance of the dryer system is not discussed in this paper.

Table 3 Average temperature and humidity in the drying chamber

No.	Sensor positions	Average Temperature (ºC)	Average Absolute Humidity (%)
1	A4 (Inlet)	56	15.9
2	A5 (Outlet)	42	22.4
3	A10 (Tray 4)	47	22.3
4	A11 (Tray 9)	42	23.5
5	A12 (Tray 11)	42	24.1
6	A13 (Tray 13)	43	24.3
7	A14 (Tray 18)	42	24.6

3D CFD simulation was conducted to predict the airflow distribution in the drying chamber because the result of a 2D simulation would not represent the real problem, as discussed by Misha et al. [19]. The product was assumed to be porous with 10% porosity. The anemometers were installed at the end of trays 4, 9, 11, 13, and 18 (sensor positions A10 to A14) for validation purposes. Unfortunately, the velocity was not recorded at all points because the anemometer range was 0.4 m/s to 30 m/s. The average air velocity at all points were lower than 0.4 m/s. The outlet velocity (A5) was recorded with an average of 8.9 m/s.

Since only one positions of the velocity can be validated (exit channel), manual measurements were carried out at the fronts of trays in column one (parallel to the center of fan 1) as shown in Fig. 10. These positions are located in the middle between upper and lower trays. However, the value of velocity at tray 2 and 3 can't be measured because the value is below 0.4 m/s. The value of measurement data and simulation result for all locations are shown in Table 5. The simulation values for all points were within the range of anemometer accuracy. Therefore, the simulation results are highly consistent with the experimental data.

Table 4 Final moisture content

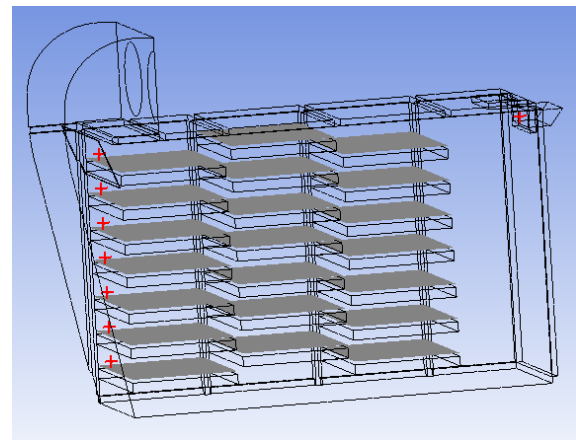| Tray position	Moisture content, % (wet basis)
4	14
9	32
11	34
13	33
18	39

Fig. 10 Position of air velocity measurement and plane above the trays

Misha et al [20] created a plane between two fans to investigate the air velocity along the tray. However, the result did not represent overall velocity for all trays and no correlation between velocity and drying rate can be concluded. In this current simulation, a plane was created 2 cm above each tray (Fig. 10) to find the average air velocity above the trays. The velocity at this region was necessary to carry the moisture from the product. The drying rate of the product at trays 4, 9, 11, 13, and 18 was determined (Table 6) from experimental result. As shown in the Fig. 11, the product with higher drying rate has higher average air velocity above the

tray as expected. The drying rate has strong correlation with average velocity above the trays. The straight line represents the relation between these two parameters, with a high R-squared value of 0.96. The equation for the straight line is given by

$$y=2.705x-0.235 \tag{5}$$

where y is the predicted drying rate and x is the air velocity from the simulation result.

Table 5 Velocity of experimental and simulation result

No.	Anemometer positions	Velocity (m/s)	
		Experiment	Simulation
1	Tray 1	0.8	0.80
2	Tray 2	-	0.15
3	Tray 3	-	0.27
4	Tray 4	0.4	0.41
5	Tray 5	0.6	0.62
6	Tray 6	0.6	0.64
7	Tray 7	0.7	0.73
8	Exit channel	8.9	9.02

Table 6 Prediction of drying rate

Tray positions	Average velocity from simulation result (m/s)	Drying rate (kg/h)	Prediction of drying rate (kg/h)	Percentage of error (%)
4	0.26	0.48	0.47	2.08
9	0.22	0.34	0.36	5.88
11	0.20	0.32	0.31	3.13
13	0.21	0.32	0.33	3.13
18	0.18	0.26	0.25	3.85
Average percentage of error				3.61

The values of the actual and predicted (using equation) drying rates are shown in Table 5. The average percentage error was extremely small and acceptable. Therefore, the drying rate at the other tray positions can be predicted by using Eq. (5). The graph in Fig. 12 shows the air velocity from the simulation and the predicted drying rate. The simulation result shows that the highest air velocity was at tray 1 and 7 because of the additional baffle and incline wall that channels the air to the each tray level. The simulation without a baffle was conducted to predict air flow in the drying chamber [21]. Without the baffle, less air was channeled to the top tray and lower air velocity was produced. The drying rate of the dried products are depend on the air velocity. The product with higher average air velocity has lower moisture content (Table 4).

Such findings also show that the incline wall at the inlet contributed to the uniform distribution of drying air to each tray level at the same column. The 3D simulation result of the air stream is shown in Fig. 13. In this study, air flow was produced by the axial fan at 1.5 m/s, which is considered high velocity and not influenced by temperature. Therefore the simulation was conducted under steady state condition. In a natural flow, air flow is depends on the temperature gradients in the air.

The simulation was simplified by assuming that the product temperature was in equilibrium with the drying air at the final stage of drying. In actual experiment the drying was stopped before this stage because the products were dried only at certain final moisture content, in this case below 15% wet basis. This simulation did not include humidity because two phases of air material are required in the process, which will result in a more complicated equation and time-consuming simulation. Instead, this study focused on predicting the air flow distribution in the drying chamber by using CFD simulation to solve Eq. (1) to (4).
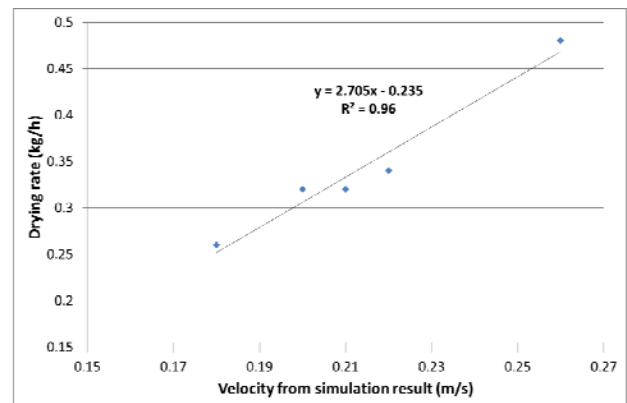

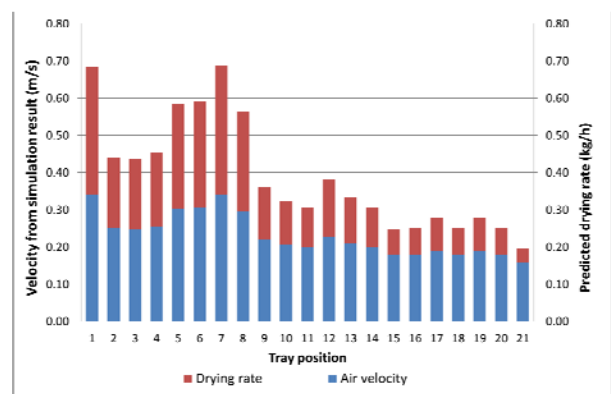Fig. 11 Drying rate against velocity from simulation.

Fig. 12 Velocity from simulation and predicted drying rate for each tray.

Based on the experimental result the airflow rate can be considered as constant along the experiment. Therefore the CFD simulation was carried out under steady state condition. Temperature was not analyzed in simulation because the temperature is not constant, fluctuate depends on solar radiation and moisture content of the dried product. Temperature analysis only can be done using transient
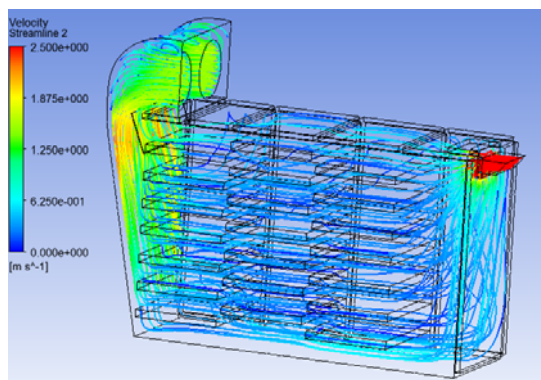
condition which is more complicated and time consuming.

Fig. 13 3D streamline in the drying chamber.

IV. CONCLUSION

A kenaf core drying experiment using a solar-assisted solid desiccant dryer was performed under average solar radiation of 834 W/m². CFD simulation was used to predict air flow distribution in the drying chamber by considering the product as porous media. The experimental and simulation data were in good agreement. The drying rate of the product was significantly influenced by the average air velocity above the tray. The higher the average air velocity, the higher the drying rate of the products. The correlation between average air velocity above the trays and drying rate at some trays is very useful to predict the drying uniformity throughout the drying chamber. As the distance of product far from the air inlet the air velocity decreased. However the uniformity of air flow distribution to each level of product at the same column are acceptable. The alternate arrangement of tray position was adopted to ensure that all trays are exposed directly to drying air. Since the products that close to the air inlet were dry earlier, drying using semi-continuous mode was recommended to shorter the drying time and improve drying uniformity.

REFERENCES

[1] S. Misha, S. Mat, M.H. Ruslan, K. Sopian, and E. Salleh, "Review on the application of a tray dryer system for agricultural products," *World Applied Sciences Journal*, vol. 22, no. 3, pp. 424–433, 2013.

[2] E. Mathioulakis, V.T. Karathanos, and V.G. Belessiotis, "Simulation of air movement in a dryer by computational fluid dynamics: Application for the drying of fruits," *Journal of Food Engineering*, vol. 36, pp.183–200, 1998

[3] P.S. Mirade, "Prediction of the air velocity field in modern meat dryers using unsteady computational fluid dynamics (CFD) models," *Journal of Food Engineering*, vol. 60, pp. 41–48, 2003.

[4] F. Pinaga, A. Mulet, A. Berna, and M. Borras, "Effect of air flow rate on carrot drying," *Drying Technology*, vol. 5, no. 2, pp. 245–258, 1987.

[5] V.G. Belessiotis and V.T. Karathanos, "Sun and artificial air drying kinetics of some agricultural products," *Journal of Food Engineering*, vol. 31, no. 1, pp. 35–46, 1997.

[6] D.P. Margaris, and A.G. Ghiaus, "Dried product quality improvement by air flow manipulation in tray dryers," *Journal of Food Engineering*, vol. 75, pp. 542–550, 2006.

[7] D.A. Tzempelikos, A.P. Vouros, A.V. Bardakas, A.E. Filios, and D.P. Margaris, "Design, construction and evaluation of a new laboratory convective dryer using CFD," *International Journal of Mechanics*, vol. 7, no. 4, pp. 425-434, 2013.

[8] B. Shao, H. Cheng, J. Li, Z. Li, L. Hou, J. Hou, and L. Wang, "Numerical simulation of complex flow field in quenching furnace with mixture of nitrogen-spray water eject quenching under normal pressure and high velocity," *International Journal of Mechanics*, vol. 3, no. 4, pp. 53-60, 2009.

[9] S. Misha, S. Mat, M.H. Ruslan, K. Sopian and E. Salleh, The Effect of Drying Air Temperature and Humidity on the Drying Kinetic of Kenaf Core, *Applied Mechanics and Materials*, vol. 315, pp.710–714, 2013.

[10] S. Misha, S. Mat, M.H. Ruslan, and K. Sopian, "Review of solid/liquid desiccant in the drying applications and its regeneration methods," *Renewable and Sustainable Energy Reviews*, no. 16, pp. 4686–4707, 2012.

[11] S. Misha, S. Mat, M.H. Ruslan, E. Salleh, and K. Sopian, "Performance of a solar assisted solid desiccant dryer for kenaf core fiber drying under low solar radiation," *Solar Energy*, no. 112, pp. 194-204, 2015.

[12] S. Misha, S. Mat, M.H. Ruslan, K. Sopian, E. Salleh, and M.A.M. Rosli, "Performance Test of Solar Assisted Solid Desiccant Dryer," *8th WSEAS International Conference on Renewable Energy Sources (RES' 14)*, Kuala Lumpur, Malaysia, 23 -25 April 2014, pp. 174-180.

[13] V.T. Karathanos, "Determination of water content of dried fruits by drying kinetics," *Journal of Food Engineering*, vol. 39, pp. 337-344, 1999.

[14] T. Norton, and D.W. Sun, "Computational fluid dynamics (CFD) – an effective and efficient design and analysis tool for the food industry: A review," *Trends in Food Science & Technology*, vol 17, pp. 600–620, 2006.

[15] O. Yongson, I.A. Badruddin , Z.A. Zainal, and P.A Aswatha Narayana, "Airflow analysis in an air conditioning room," *Building and Environment*, vol. 42, pp. 1531–1537, 2007.

[16] P. Chuchard, T. Puapansawat, T. Siriapisith, Y.H. Wu, and B. Wiwatanapataphee, "Numerical simulation of blood flow through the system of coronary arteries with diseased left anterior descending," *International Journal of Mathematics and Computers in Simulation*, vol. 5, no. 4, pp. 334-341, 2011.

[17] S. Misha, S. Mat, M.H. Ruslan, K. Sopian, and E. Salleh, "Comparison of CFD Simulation on Tray Dryer System Between Porous and Solid Product," *7th WSEAS International Conference on Renewable Energy Sources (RES' 13)*, Kuala Lumpur, Malaysia, 2-4 April 2013, pp. 59-64.

[18] D.A. Tzempelikos, A.P. Vouros, A.V. Bardakas, A.E. Filios, and D.P. Margaris, "Analysis of air velocity distribution in a laboratory batch-type tray air dryer by computational fluid dynamics," *International Journal of Mathematics and Computers in Simulation*, vol. 6, no. 5, pp. 413-421, 2012.

[19] S. Misha, S. Mat, M.H. Ruslan, K. Sopian, and E. Salleh, "Comparison between 2D and 3D simulations of a tray dryer system using CFD software," *World Applied Sciences Journal*, vol. 29, no. 10, pp. 1301–1309, 2014.

[20] S. Misha, S. Mat, M.H. Ruslan, K. Sopian, and E. Salleh, "The CFD simulation of tray dryer design for kenaf core drying," *Applied Mechanics and Materials*, vol. 393, pp. 717-722, 2013.

[21] S. Misha, S. Mat, M.H. Ruslan, K. Sopian, and E. Salleh, "The prediction of drying uniformity in tray dryer system using CFD simulation," *International Journal of Machine Learning and Computting*, vol. 3, no.5, pp. 419–423, 2013.